

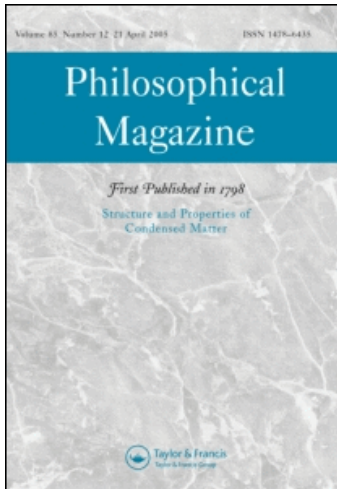
This article was downloaded by: [Aly, K. A.]

On: 28 April 2009

Access details: Access Details: [subscription number 910707206]

Publisher Taylor & Francis

Informa Ltd Registered in England and Wales Registered Number: 1072954 Registered office: Mortimer House, 37-41 Mortimer Street, London W1T 3JH, UK



Philosophical Magazine

Publication details, including instructions for authors and subscription information:

<http://www.informaworld.com/smpp/title-content=t713695589>

Optical constants of quaternary Ge-As-Te-In amorphous thin films evaluated from their reflectance spectra

K. A. Aly ^a

^a Faculty of Science, Department of Physics, Al Azhar University, Assiut, Egypt

Online Publication Date: 01 April 2009

To cite this Article Aly, K. A. (2009) 'Optical constants of quaternary Ge-As-Te-In amorphous thin films evaluated from their reflectance spectra', *Philosophical Magazine*, 89:12, 1063 — 1079

To link to this Article: DOI: 10.1080/14786430902870542

URL: <http://dx.doi.org/10.1080/14786430902870542>

PLEASE SCROLL DOWN FOR ARTICLE

Full terms and conditions of use: <http://www.informaworld.com/terms-and-conditions-of-access.pdf>

This article may be used for research, teaching and private study purposes. Any substantial or systematic reproduction, re-distribution, re-selling, loan or sub-licensing, systematic supply or distribution in any form to anyone is expressly forbidden.

The publisher does not give any warranty express or implied or make any representation that the contents will be complete or accurate or up to date. The accuracy of any instructions, formulae and drug doses should be independently verified with primary sources. The publisher shall not be liable for any loss, actions, claims, proceedings, demand or costs or damages whatsoever or howsoever caused arising directly or indirectly in connection with or arising out of the use of this material.

Optical constants of quaternary Ge–As–Te–In amorphous thin films evaluated from their reflectance spectra

K.A. Aly*

Faculty of Science, Department of Physics, Al Azhar University, Assiut, Egypt

(Received 31 March 2008; final version received 4 March 2009)

Thin films of amorphous $\text{Ge}_9\text{As}_{20}\text{Te}_{71-x}\text{In}_x$ with different compositions ($x = 0, 3, 6$ and 9 at. %) were obtained by deposition onto glass substrates by thermal evaporation. The reflection spectra, $R(\lambda)$, of the films were obtained in the spectral region from 400 to 2500 nm. A straightforward analysis proposed by Ruiz-Perez et al., based on the use of the maxima and minima of the interference fringes, has been applied to derive the real and imaginary parts of the complex index of refraction, the thickness and the thickness variation of the studied films. Increasing In content is found to affect the refractive index and the extinction coefficient of the films. Optical absorption measurements were used to obtain the fundamental absorption edge as a function of composition. With increasing In content, the refractive index decreases, whereas the optical band gap, E_g , increases. The relationship between E_g and the chemical composition of the $\text{Ge}_9\text{As}_{20}\text{Te}_{71-x}\text{In}_x$ system is discussed in terms of the cohesive energy, the average heat of atomization, H_s , and the average coordination number, N_c .

Keywords: optical constant; amorphous thin film; band gap; absorption edge

1. Introduction

Chalcogenide glasses are an important class of amorphous semiconductors, and studies of optical properties of these glasses are essential for fundamental reasons and from an applications point of view [1,2]. They have recently attracted a great deal of interest because of their many applications as solid-state devices [3]. A common feature of these glasses is the presence of localized states in the mobility gap as a result of the absence of long-range order as well as various inherent defects. Investigation of electronic transport in disordered systems has been gradually developed and the investigation of gap states is of particular interest because of their effect on the electrical properties of semiconductors [4]. Current interest in chalcogenide materials centers on X-ray imaging and photonics [5]. The optical band gap, refractive index and extinction coefficient are significant parameters in amorphous thin films. A high refractive index and a low extinction coefficient provide strong electromagnetic field confinement with low absorption loss. This makes chalcogenide glasses useful for the fabrication of optical nanofibers in which

*Email: kamalaly2001@gmail.com

light experiences strong non-linearities due to a small effective mode area associated with evanescent fields just outside the fiber surface. The evanescent wave from a chalcogenide-based optical fiber is used in biological sensing applications [6]. Telluride glasses have been widely investigated for their application as switching and memory devices. The switching behavior arises from a glass-to-crystal transition during the application of current or on heating [7–9]. Because of this interest, a number of papers reporting the electrical properties, photoconductivity, glass formation, structure and crystallization kinetics of Ge–As–Te glasses have appeared in the literature [10–15].

Various workers have studied the optical properties and great efforts have been made to develop the mathematical formulation describing the transmittance and reflectance of different systems [16–24]. Many theoretical methods dealing with films showing thickness variations can be found in the literature [18,22,24]. Furthermore, the calculation algorithms suggested have been applied successfully to characterize geometrically and optically thin dielectric films showing a linear thickness variation [24–26]. Reflectometry in the spectral intervals covering the UV, visible and near infrared (UV/vis/NIR) intervals, yields valuable information about any non-uniform thickness in the films. In the present work, the methods of Minkov [20,24] and Ruiz-Perez et al. [27], which are based only on the use of the two envelopes containing the maxima and minima of reflection spectra, has been used in order to study the effect of In additions on the optical constants, calculate the optical constants, the thickness and the thickness variations of thermally evaporated $\text{Ge}_9\text{As}_{20}\text{Te}_{71-x}\text{In}_x$ ($x=0, 3, 6$ and 9 at. %) thin films.

2. Theoretical basis of the method

Consider an optical system composed of a thin isotropic film with refractive index n and extinction coefficient k (or absorption coefficient α) deposited onto a substrate whose thickness d_s is several orders of magnitude larger than the thickness of the film d and whose refractive index n_s is larger than the refractive index of the film. The two-layer optical system is surrounded by air. The interference phenomenon stemming from multiple reflections at the dielectric–film interface are resolved by the experimental measurement system ($\Delta\lambda \ll \lambda^2/2nd$), whereas those occurring at the substrate interface cannot be discriminated by the instrument owing to the spectral distribution of the probe light ($\Delta\lambda \gg \lambda^2/2n_s d_s$). The light used to measure the optical reflectance of this system, with mean wavelength λ and spectral half width $\Delta\lambda$, is incidentally normally on the film surface.

If the above assumptions are all satisfied, and the thickness of the dielectric film is uniform, the reflectance of such a two-layer system, at a wavelength λ , can be expressed in the case where $k^2 \ll n_s^2 < n^2$ as follows [20,22]:

$$R = \frac{A}{B} + \frac{g x_a^2}{BC}, \quad (1)$$

where $A = (ad)^2 + (bcx_a)^2 - 2abcdx_a \cos(\phi)$, $B = (bd)^2 + (acx_a)^2 - 2abcdx_a \cos(\phi)$, $C = (b^3f) + (a^3ex_a^2) - 2abcdx_a \cos(\phi)$, $a = n - 1$, $b = n + 1$, $c = n - n_s$, $d = n + n_s$, $e = n - n_s^2$, $f = n + n_s^2$, $g = 64n_s(n_s - 1)^2 n^4$, $x_a = \exp(-\alpha d)$, $\phi = 4\pi nd/\lambda$, $\alpha = 4\pi k/\lambda$ and

$n_s = (1 + \sqrt{R_s(2 - R_s)})/(1 - R_s)$, where R_s is the measured substrate reflection and x_a is the film absorbance.

Integrating Equation (1) over the thickness d , or equivalently over the phase ϕ , gives us the formula for the reflectance R_Δ of a wedge-shaped film [22,24] that is characterized by an average thickness \bar{d} larger than the thickness variation Δd , which is the actual variation in thickness at the extreme of the illuminated area, i.e. the thickness can be expressed as $d \pm \Delta d$,

$$R_{\Delta d} = \frac{1}{\phi_2 - \phi_1} \int_{\phi_1}^{\phi_2} \left[\frac{A}{B} + \frac{gx^2}{B \cdot C} \right] d\phi = \frac{1}{2\Delta d} \int_{d_1}^{d_2} \left[\frac{A}{B} + \frac{gx^2}{B \cdot C} \right] dd, \quad (2)$$

where $\phi_1 = 2\pi n(\bar{d} - \Delta d)/\lambda$ and $\phi_2 = 2\pi n(\bar{d} + \Delta d)/\lambda$.

Equation (2) can be solved by taking into account the basic equation for the interference fringes [17–19]:

$$2n\bar{d} = m\lambda_{\tan}, \quad (3)$$

where λ_{\tan} is the wavelength corresponding to tangent points between the reflectance spectrum and its upper and lower envelopes, and the order number m is an integer for minima and a half-integer for maxima of the reflection spectra, $R_{\Delta d}$. Then one can write an analytical expression for the lower and upper envelopes [20,21,23] as a function of n , x_a , Δd as

$$R_{\Delta m} = R_{\Delta m}(n, x_a, \Delta d), \quad R_{\Delta M} = R_{\Delta M}(n, x_a, \Delta d). \quad (4)$$

The range of validity of the system of Equations (4) is $0 < \Delta d < \lambda/4n$.

3. Experimental details

Chalcogenide glasses of the $\text{Ge}_9\text{As}_{20}\text{Te}_{71-x}\text{In}_x$ ($x=0, 3, 6$ and 9 at. %) system were prepared from Ge, As, Te and In elements with high purity (99.999%) by the usual melt quenching technique. Materials were weighed according to their atomic percentages, charged into cleaned silica tubes and then sealed under a vacuum of 1.33×10^{-3} Pa. The ampoules were put into a furnace at around 1250 K for 24 h. During the heating process, the ampoules were shaken several times to maintain their homogeneity, then the ampoules were quenched in ice-cooled water to avoid crystallization. Thin films were prepared by thermal evaporation of small ingot pieces onto electronically cleaned glass substrates (microscope slides). The thermal evaporation process was performed by using a coating system (Denton Vacuum 502 A), at a pressure of approximately 1.33×10^{-3} Pa during the deposition process. The thickness of the film was determined using a quartz crystal monitor (Denton model DTM-100). The rate of the film deposition, which was controlled using the same DTM-100 quartz crystal monitor, was $1\text{--}10 \text{ \AA s}^{-1}$. The $\text{Ge}_9\text{As}_{20}\text{Te}_{71-x}\text{In}_x$ thin films had thicknesses in the range of 850–990 nm.

The elemental compositions of the investigated specimens were checked using energy-dispersive X-ray (Link Analytical Edx) spectroscopy. The deviations in the elemental compositions of the evaporated thin films from their initial bulk specimens were found to be ± 0.37 at. %. The amorphous state of the films was checked using an X-ray (Philips

type 1710 with Cu as a target and Ni as a filter, $\lambda = 1.5418 \text{ \AA}$) diffractometer. The absence of crystalline peaks confirmed the amorphous state of the prepared samples.

The optical reflectance was measured using a double-beam computer-controlled spectrophotometer (Shimadzu 2101 UV-VIS), at normal incidence and in the wavelength range 400–2500 nm. The two envelopes, $R_{\Delta m}$ and $R_{\Delta M}$, were drawn around the extremes for each reflectance spectrum using the Origin version 7 program (Origin Lab Corp). Figure 1 shows the measured reflectance $R_{\Delta d}$ spectra and the created envelopes, $R_{\Delta M}$ and $R_{\Delta m}$, for different compositions of $\text{Ge}_9\text{As}_{20}\text{Te}_{71-x}\text{In}_x$ ($x=0, 3, 6$ and 9 at. %) thin films. The physical parameters (coordination number N_r , average heats of atomization H_s (kcal/g atom), electronegativity, χ , bond energy [28–32]) of the constituent elements are listed in Table 1.

4. Results and discussion

4.1. Determination of refractive index, film thickness and the thickness variation

Taking into account that the absorbance $x=1$ in the transparent region, then the two transcendental Equations (4) can be solved for n and Δd at every tangent point λ_{tan} between the reflection spectrum and its two envelopes. These n values are denoted by n_1 , as shown in Table 2. The final value of the wedging parameter $\overline{\Delta d}$ is determined by averaging a certain set of Δd values showing a low scattering (see Table 2). After the determination of accurate values Δd , the two Equations (4) are solved again to obtain the next approximations for n_2 and x_1 at each value of λ_{tan} . The experimental errors in $R_{\Delta m}$, $R_{\Delta M}$ significantly decrease the accuracy of these n_2 values calculated from Equations (4) [24]. If $n''_{1(2)}$ and $n'_{1(2)}$ are the refractive indices belonging to the set of n_1 or n_2 values at two adjacent maxima (or minima) at λ' and λ'' , then the film thickness d_1 or d_2 can be expressed as

$$d_{(1 \text{ or } 2)} = \frac{\lambda' \lambda''}{2(n''_{1 \text{ or } 2} \lambda'_1 - n'_{1 \text{ or } 2} \lambda''_1)}. \quad (5)$$

The values of d determined by Equation (5) for different samples are listed as d_1 in Table 2. Hence, an initial approximate value of the thickness \bar{d}_1 , or a new improved value of \bar{d}_2 , can be calculated by Equation (5). Substituting \bar{d}_1 or \bar{d}_2 and the corresponding values of n_1 or n_2 into Equation (3) gives the order number for a given tangent point m_1 . The final film thickness of the non-uniform film $\bar{d}(=d_3)$ is determined by averaging the value for d_3 calculated by Equation (3) (see Table 2), where the values of n_1 or n_2 , as well as their corresponding m values, are used. Furthermore, a simple complementary graphical method for deriving the first-order number m_1 and the final film thickness d , based on Equation (3), was also used. For this purpose, Equation (3) is rewritten [17–19] as follows for the successive maxima and minima, starting from the long-wavelength end:

$$\frac{l}{2} = 2d \cdot \left(\frac{n}{\lambda}\right) - m_1, \quad l = 0, 1, 2, 3, \dots, \quad (6)$$

where m_1 is the order number of the first ($l=0$) extrema considered; m_1 is integer for a minima and half-integer for a maxima and d is the film thickness. Therefore, a plot

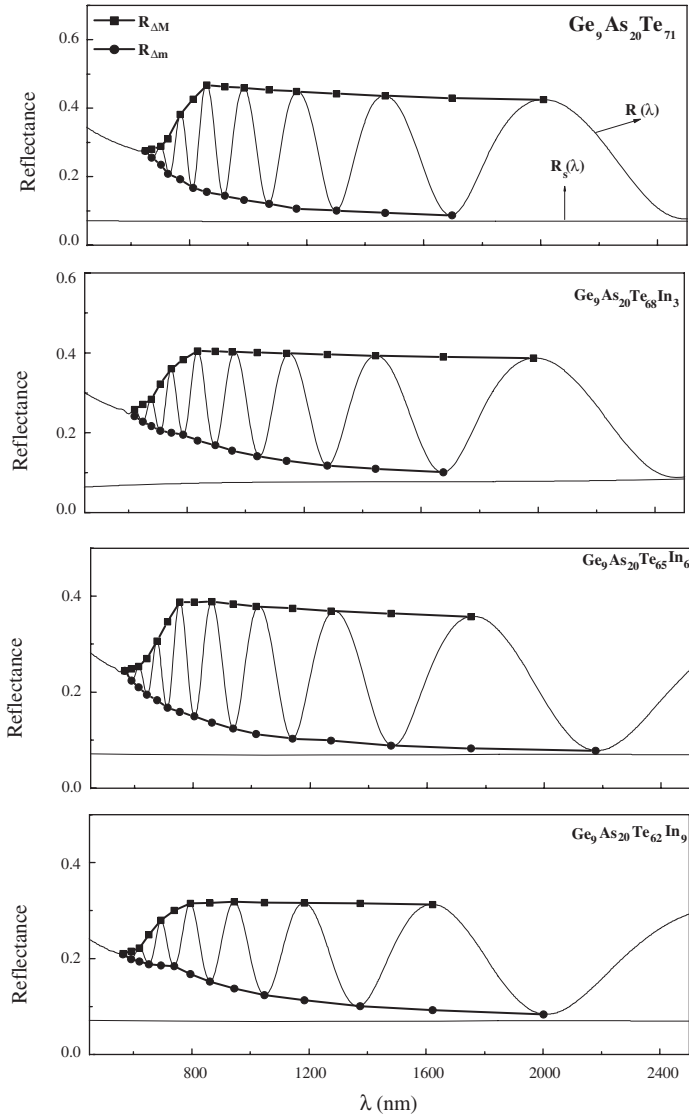


Figure 1. Reflectance spectra of four different wedge-shaped films of $\text{Ge}_9\text{As}_{20}\text{Te}_{71-x}\text{In}_x$ ($x = 0, 3, 6$ and 9 at. %) deposited onto thick transparent substrates. The values of $R_{\Delta M}$ and $R_{\Delta m}$ refer to the upper and lower envelopes, respectively. R_s is the reflectance of the substrate alone.

of $l/2$ versus n/λ yields a straight line with slope $2d$ where $d = \text{slope}/2$ and a cut-off on the vertical axis at $-m_1$. Figure 2 shows this plot, from which the values obtained for $2d$ and m_1 are displayed for each sample investigated. It is worth noting that the exact value of the first orders m_1 of the order number m and the average film thickness $\bar{d}(=\bar{d}_3)$ given in Table 2 are found to be in agreement with those obtained from Figure 2.

Table 1. Physical parameters of the constituent elements.

Property	Ge	As	Te	In
Coordination number [18,19]	4	3	2	3
H_s (kcal/g atom) [20]	90	69.0	46.0	58
Electronegativity [19,21]	1.8	2.18	2.1	1.7
Bond energy (kcal mol ⁻¹) [19,22]	65.48	32.10	33	24.2

The final values of the refractive index $n(=n_3)$ are obtained at each tangent point from Equation (3) by substituting \bar{d} and m . Now, the values of n_3 can be fitted to a function such as the two-term Cauchy dispersion relationship, $n(\lambda) = a + b/\lambda^2$, which can then be used to extrapolate the wavelength dependence beyond the range of measurement [33] (see Figure 3). The least-squares fit of the four sets of values of n_3 for the different samples listed in Table 2 yields $n = 2.58 + (2.7 \times 10^5/\lambda^2)$, $n = 2.466 + (2.08 \times 10^5/\lambda^2)$, $n = 2.352 + (1.99 \times 10^5/\lambda^2)$ and $n = 2.225 + (1.5 \times 10^5/\lambda^2)$ for $\text{Ge}_9\text{As}_{20}\text{Te}_{71-x}\text{In}_x$ with compositions $x = 0, 3, 6$ and 9 at. %, respectively.

The final values of the refractive index can be fitted to an appropriate function such as the Wemple–DiDomenico (WDD) dispersion relationship [34], i.e. to the single-oscillator model,

$$n^2(h\nu) = 1 + \frac{E_o E_d}{E_o^2 - (h\nu)^2}, \quad (7)$$

where E_o is the single-oscillator energy and E_d is the dispersion energy or single-oscillator strength. By plotting $(n^2 - 1)^{-1}$ against $(h\nu)^2$ and fitting straight lines, as shown in Figure 4, E_o and E_d can be determined from the intercept (E_o/E_d) and the slope $(E_o E_d)^{-1}$. The oscillator energy E_o is an average energy gap and, to a good approximation, scales with the optical band gap E_g , $E_o \approx 2E_g$ [35]. Figure 4 also shows the values of the refractive index $n(0)$ at $h\nu = 0$ of the $\text{Ge}_9\text{As}_{20}\text{Te}_{71-x}\text{In}_x$ films. The obtained values of E_o , E_d and $n(0)$ are listed in Table 3.

It can be observed that the single-oscillator energy E_o increases with increasing In content, whereas the refractive index $n(0)$ and the dispersion energy E_d decrease. An important achievement of the WDD model is that it relates the dispersion energy E_d to other physical parameters of the material through the following empirical relationship [34] $E_d = \beta N_c Z_a N_e$ eV, where N_c is the effective coordination number of the cation nearest-neighbor to the anion, Z_a is the formal chemical valence of the anion, N_e is the effective number of valence electrons per anion and β is a two-valued constant with either an ionic or a covalent value ($\beta_i = 0.26 \pm 0.03$ eV and $\beta_c = 0.37 \pm 0.04$ eV, respectively). Therefore, in order to account for the compositional trend of E_d , it is suggested that the observed decrease in E_d with increasing In content is primarily due to the change in the ionicities (homopolar Te–Te bonds are introduced together with extra In atoms), which increases with the In content. The values of the single-oscillator energy, the dispersion energy, the static refractive index and the excess of Te–Te homopolar bonds for the $\text{Ge}_9\text{As}_{20}\text{Te}_{71-x}\text{In}_x$ thin films are listed in Table 3.

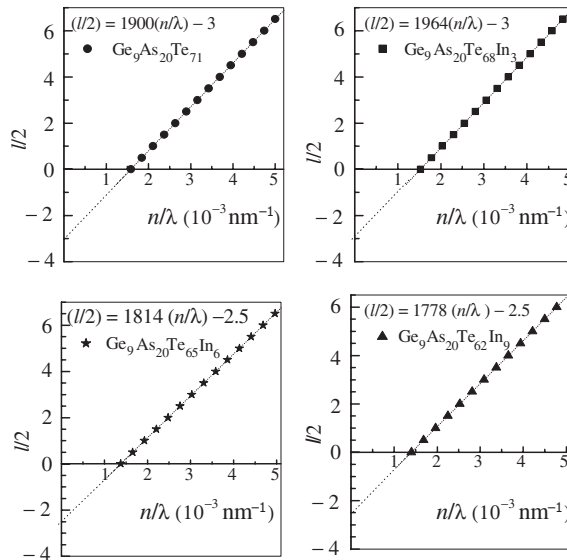
Table 2. Values of λ , $R_{\Delta M}$ and $R_{\Delta m}$ for $\text{Ge}_9\text{As}_{20}\text{Te}_{71-x}\text{In}_x$ ($x=0, 3, 6$ and 9 at.%) films from the reflectance spectra of Figure 1. The underlined reflectance values are those given in the spectra of Figure 1 and the others are calculated by the envelope method. The wedging parameter, the average thickness and the absorbance were determined by Minkov's method. It is worth noting that the exact value of the first orders m_1 and the average film thickness are found to be in agreement with those obtained by Equation (6) (see Figure 2).

Sample	λ	$R_{\Delta M}$	$R_{\Delta m}$	n_1	Δd (nm)	d_2 (nm)	m	d_3 (nm)	n_3	x_{a1}	x_{a2}
$\text{Ge}_9\text{As}_{20}\text{Te}_{71}$	1698	0.430	<u>0.087</u>	2.665	37.3	1047	3	930	2.681	0.913	~1
	1468	<u>0.436</u>	0.094	2.696	35.7	1081	3.5	929	2.704	0.920	~1
	1302	<u>0.442</u>	<u>0.101</u>	2.728	34.2	946	4	938	2.741	0.942	~1
	1166	<u>0.449</u>	<u>0.107</u>	2.762	<u>32.0</u>	—	4.5	950	2.762	1.000	~1
	1072	<u>0.454</u>	<u>0.12</u>	2.801	<u>32.7</u>	—	5	950	2.821	0.980	~1
	986	<u>0.459</u>	<u>0.132</u>	2.839	<u>32.4</u>	—	5.5	952	2.854	0.992	~1
	920	<u>0.463</u>	<u>0.144</u>	2.875	<u>32.1</u>	—	6	960	2.905	1.000	~1
	858	<u>0.467</u>	<u>0.156</u>	2.912	<u>31.6</u>	—	6.5	968	2.935	1.029	0.836
	812	<u>0.426</u>	<u>0.167</u>	2.792	<u>36.0</u>	—	7	964	2.992	0.838	0.602
	768	<u>0.382</u>	<u>0.193</u>	2.713	43.2	—	7.5	941	3.032	0.604	0.337
	726	<u>0.311</u>	<u>0.209</u>	2.558	53.6	—	8	966	3.057	0.338	0.183
	702	<u>0.289</u>	<u>0.235</u>	2.577	58.9	—	8.5	971	3.141	0.184	0.094
	670	<u>0.281</u>	<u>0.255</u>	2.618	59.7	—	9	960	3.17	0.095	0.004
	648	<u>0.276</u>	<u>0.275</u>	2.669	60.54	—	9.5	959	3.24	0.0039	
	$\overline{\Delta d} = 32.2 \pm 0.42(1.3\%) \text{ nm}$, $\overline{d_2} = 1025 \pm 70(6.8\%) \text{ nm}$, $\overline{d_3} = 953 \pm 14(1.5\%) \text{ nm}$										
$\text{Ge}_9\text{As}_{20}\text{Te}_{68}\text{In}_3$	1676	0.39	<u>0.101</u>	2.566	47.80	1021	3	952	2.56	0.899	~1
	<u>1444</u>	<u>0.393</u>	0.11	2.590	46.02	1039	3.5	951	2.57	0.915	~1
	<u>1280</u>	<u>0.396</u>	<u>0.118</u>	2.614	<u>43.99</u>	1052	4	966	2.607	0.956	~1
	<u>1140</u>	<u>0.399</u>	<u>0.13</u>	2.646	<u>43.39</u>	1106	4.5	961	2.612	0.970	~1
	<u>1040</u>	<u>0.401</u>	<u>0.141</u>	2.673	<u>42.44</u>	1078	5	974	2.648	1.005	~1
	<u>954</u>	<u>0.403</u>	<u>0.155</u>	2.708	<u>42.10</u>	—	5.5	976	2.672	1.022	~1
	<u>896</u>	<u>0.404</u>	<u>0.169</u>	2.740	<u>41.78</u>	—	6	982	2.707	1.04	~1
	<u>836</u>	<u>0.405</u>	<u>0.181</u>	2.770	<u>40.88</u>	—	6.5	1012	2.767	1.097	0.909
	<u>786</u>	<u>0.383</u>	<u>0.195</u>	2.735	<u>43.40</u>	—	7	992	2.801	0.957	0.811
	<u>746</u>	<u>0.36</u>	<u>0.2</u>	2.681	<u>45.05</u>	—	7.5	1005	2.849	0.875	0.628
	<u>708</u>	<u>0.322</u>	<u>0.205</u>	2.588	49.09	—	8	1006	2.884	0.692	0.398
	<u>678</u>	<u>0.284</u>	<u>0.217</u>	2.523	55.15	—	8.5	999	2.934	0.438	0.288
	<u>648</u>	<u>0.271</u>	<u>0.228</u>	2.522	56.56	—	9	997	2.969	0.331	0.115
	<u>620</u>	<u>0.258</u>	<u>0.242</u>	2.532	58.35	—	9.5	987	2.999	0.156	
	$\overline{\Delta d} = 43 \pm 1.1(2.6\%) \text{ nm}$, $\overline{d_2} = 1059 \pm 33.4(3.2\%) \text{ nm}$, $\overline{d_3} = 983 \pm 20.2(2.1\%) \text{ nm}$										
$\text{Ge}_9\text{As}_{20}\text{Te}_{65}\text{In}_6$	1750	<u>0.358</u>	0.083	2.504	45.890	981	2.5	874	2.412	0.872	~1
	1476	<u>0.364</u>	<u>0.088</u>	2.515	42.198	1106	3	883	2.448	0.899	~1
	1272	<u>0.369</u>	<u>0.099</u>	2.569	42.395	924	3.5	873	2.474	0.874	~1
	1140	<u>0.375</u>	<u>0.103</u>	2.542	<u>38.74</u>	1020	4	897	2.514	0.949	~1
	1016	<u>0.379</u>	<u>0.113</u>	2.556	<u>37.90</u>	—	4.5	900	2.535	0.971	~1
	936	<u>0.384</u>	<u>0.124</u>	2.577	<u>37.35</u>	—	5	908	2.58	0.992	~1
	864	<u>0.389</u>	<u>0.137</u>	2.605	<u>37.01</u>	—	5.5	912	2.620	1.008	~1
	804	<u>0.388</u>	<u>0.15</u>	2.635	<u>37.18</u>	—	6	915	2.66	1.000	~1
	754	<u>0.388</u>	<u>0.159</u>	2.618	<u>36.43</u>	—	6.5	936	2.702	1.044	0.964
	712	<u>0.347</u>	<u>0.168</u>	2.69	40.943	—	7	926	2.748	0.817	0.77
	676	<u>0.307</u>	<u>0.183</u>	2.761	46.945	—	7.5	918	2.795	0.584	0.562
	642	<u>0.27</u>	<u>0.195</u>	2.778	52.567	—	8	924	2.831	0.379	0.328
	614	<u>0.254</u>	<u>0.21</u>	2.882	55.319	—	8.5	905	2.877	0.245	0.184
	590	<u>0.249</u>	<u>0.224</u>	2.878	55.815	—	9	923	2.927	0.157	0.099

(continued)

Table 2. Continued.

Sample	λ	$R_{\Delta M}$	$R_{\Delta m}$	n_1	Δd (nm)	d_2 (nm)	m	d_3 (nm)	n_3	x_{a1}	x_{a2}
$\overline{\Delta d} = 37.44 \pm 0.80(2.1\%) \text{ nm}$, $\overline{d_2} = 1008 \pm 76.45(7.6\%) \text{ nm}$, $\overline{d_3} = 907 \pm 19.5(2.1\%) \text{ nm}$											
Ge ₉ As ₂₀ Te ₆₂ In ₉	1622	<u>0.313</u>	0.092	2.298	60.028	940	2.5	850	2.281	0.852	~1
	1374	<u>0.315</u>	<u>0.100</u>	2.319	56.347	961	3	865	2.318	0.890	~1
	1184	<u>0.316</u>	<u>0.113</u>	2.346	55.259	893	3.5	860	2.331	0.898	~1
	1048	<u>0.317</u>	<u>0.123</u>	2.369	<u>52.764</u>	—	4	877	2.358	0.968	~1
	944	<u>0.318</u>	<u>0.137</u>	2.401	<u>51.819</u>	—	4.5	886	2.389	1.007	~1
	862	<u>0.316</u>	<u>0.152</u>	2.429	<u>51.503</u>	—	5	893	2.424	1.024	~1
	794	<u>0.315</u>	<u>0.168</u>	2.463	<u>50.927</u>	—	5.5	890	2.456	1.058	~1
	740	<u>0.300</u>	<u>0.184</u>	2.463	<u>52.818</u>	—	6	890	2.497	0.954	0.955
	694	<u>0.28</u>	<u>0.186</u>	2.417	<u>53.441</u>	—	6.5	913	2.537	0.918	0.918
	652	<u>0.25</u>	<u>0.188</u>	2.348	56.401	—	7	915	2.567	0.753	0.753
	620	<u>0.222</u>	<u>0.194</u>	2.297	61.014	—	7.5	906	2.615	0.476	0.476
	592	<u>0.215</u>	<u>0.199</u>	2.294	60.830	—	8	916	2.664	0.419	0.42
	564	<u>0.21</u>	<u>0.209</u>	2.310	60.757	—	8.5	898	2.696	0.186	0.187
$\overline{\Delta d} = 52.2 \pm 0.95(1.8\%) \text{ nm}$, $\overline{d_2} = 931 \pm 35(3.8\%) \text{ nm}$, $\overline{d_3} = 889 \pm 21(2.4\%) \text{ nm}$											

Figure 2. Plot of $l/2$ versus n/λ in order to determine m_1 and d for Ge₉As₂₀Te_{71-x}In_x ($x = 0, 3, 6$ and 9 at. %) films.

The dependence of the refractive index n on the lattice dielectric constant ε_L is given by [36]

$$n^2 = \varepsilon_L - \left(\frac{e^2}{\pi c^2}\right) \left(\frac{N}{m^*}\right) \lambda^2, \quad (8)$$

where N/m^* is the ratio of the carrier concentration N to the effective mass m^* , c is the speed of light and e is the electronic charge. Plots of n^2 versus λ^2 , as shown in Figure 5, are linear, verifying Equation (8). The values of ε_L and N/m^* were deduced

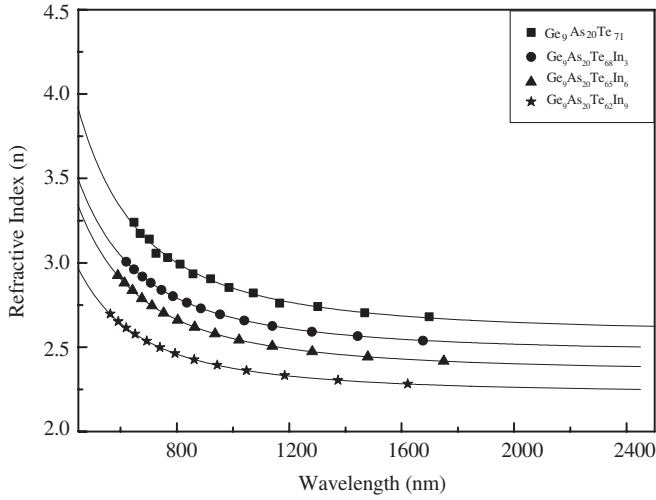


Figure 3. The refractive index, n , as a function of wavelength, λ , for different compositions of $\text{Ge}_9\text{As}_{20}\text{Te}_{71-x}\text{In}_x$ ($x = 0, 3, 6$ and 9 at. %) thin films. Solid curves are determined according to the two-term Cauchy dispersion relationship, $n(\lambda) = a + b/\lambda^2$.

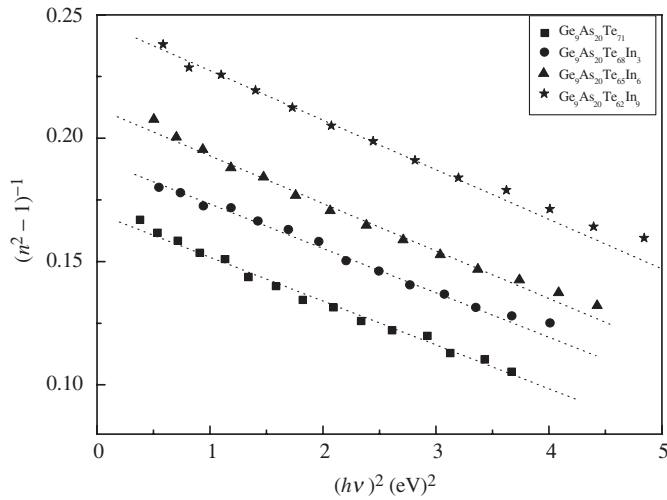


Figure 4. Plots of refractive index factor $(n^2 - 1)^{-1}$ versus $(h\nu)^2$ for different compositions of $\text{Ge}_9\text{As}_{20}\text{Te}_{71-x}\text{In}_x$ ($x = 0, 3, 6$ and 9 at. %) films.

from the extrapolation of these plots to $\lambda^2 = 0$ and from the slope of the graph, respectively (see Table 3).

4.2. Determination of the absorption coefficient and the optical band gap

Since the values of the final film thickness, \bar{d} , the thickness variations, $\Delta\bar{d}$, and refractive index, n , are already known over the whole spectral range 400–2500 nm,

Table 3. Calculated values of the average coordination number, N_r , the number of constraints, N_s ($N_s = N^\alpha + N^\beta$), the excess of Te-Te homopolar bonds, the cohesive energy (CE), the average heat of atomization, H_s^* , the dispersion parameters [E_0 , E_d and $n(0)$], the N/m^* ratio and lattice dielectric constant, ϵ_L , for different compositions of $\text{Ge}_9\text{As}_{20}\text{Te}_{71-x}\text{In}_x$ ($x=0, 3, 6$ and 9 at. %) films.

In (at. %)	N_r	N_s	N^α	N^β	Te-Te bonds	CE (eV atom ⁻¹)	H_s^* (kcal g ⁻¹)	E_0 (eV)	E_d (eV)	$N(0)$	N/m^* ($\times 10^{-37}$ cm ⁻¹)	ϵ_L
0	2.38	2.95	1.19	1.76	23	1.73	27.28	3.16	18.60	2.62	10.43	7.4
3	2.47	3.18	1.24	1.94	15	1.75	27.46	3.26	17.06	2.50	9.9	6.7
6	2.56	3.40	1.28	2.12	8	1.78	27.64	3.34	15.76	2.39	8.8	6.1
9	2.65	3.63	1.33	2.30	—	1.80	27.82	3.51	14.23	2.25	6.6	5.4

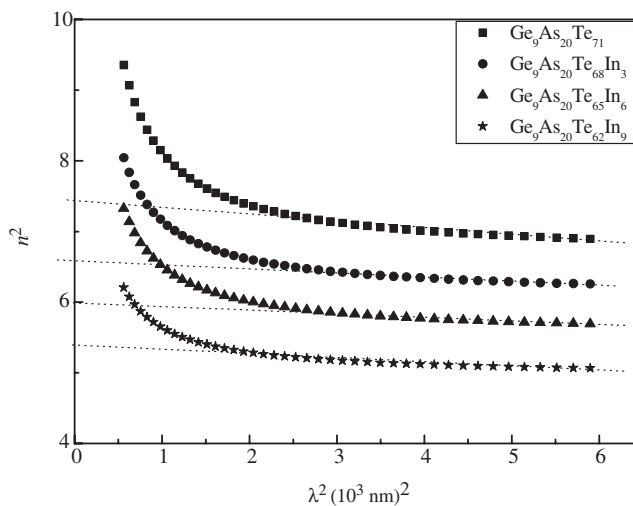


Figure 5. Plots of refractive index squared n^2 versus $(h\nu)^2$ for different compositions of $\text{Ge}_9\text{As}_{20}\text{Te}_{71-x}\text{In}_x$ ($x=0, 3, 6$ and 9 at. %) films.

the absorbance $x_a(\lambda)$ can be obtained by solving Equation 4 for the upper envelope $R_{\Delta M}$ [24]. When the absorbance is known, the relation $x_a = \exp(-4\pi kd/\lambda) = \exp(-\alpha d)$ can then be solved for the values of the absorption coefficient α or the extinction coefficient k in order to complete the calculation of the optical constants. Figure 6 illustrates the dependence of k on the wavelength for different compositions of $\text{Ge}_9\text{As}_{20}\text{Te}_{71-x}\text{In}_x$ ($x=0, 3, 6$ and 9 at. %) thin films.

As shown in Figure 6, the absorption coefficient, α , or the extinction coefficient, $k = \alpha\lambda/4\pi$, decreases (i.e. there is a blue shift of the optical absorption edge) with increasing In content. According to Tauc's relation [37,38], for larger values of the absorption coefficient ($\alpha \geq 10^4$ cm⁻¹), the photon energy dependence of the absorption coefficient can be described by the formula

$$(\alpha h\nu)^{1/2} = B(h\nu - E_g), \quad (9)$$

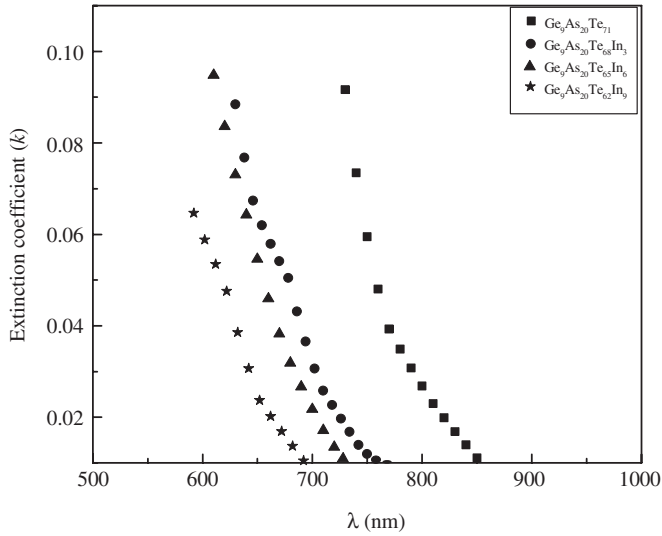


Figure 6. Extinction coefficient, k , versus wavelength, λ , for $\text{Ge}_9\text{As}_{20}\text{Te}_{71-x}\text{In}_x$ ($x = 0, 3, 6$ and 9 at. %) films.

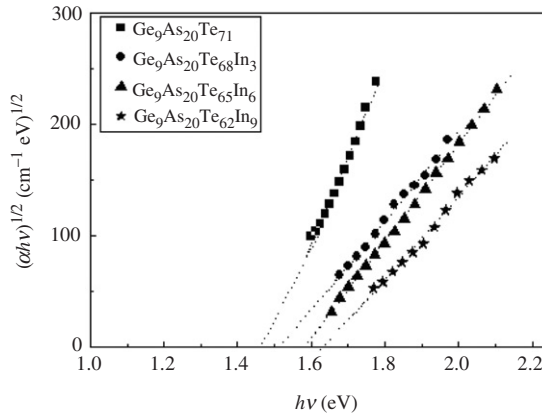


Figure 7. Dependence of $(\alpha hv)^{1/2}$ on photon energy ($h\nu$) for the different composition of amorphous $\text{Ge}_9\text{As}_{20}\text{Te}_{71-x}\text{In}_x$ ($x = 0, 3, 6$ and 9 at. %) films, from which the optical band gap, E_g , is estimated (Tauc extrapolation).

where B is a parameter that depends on the transition probability and E_g is the optical energy gap. Figure 7 is a typical best fit of $(\alpha hv)^{1/2}$ versus photon energy ($h\nu$) for the $\text{Ge}_9\text{As}_{20}\text{Te}_{71-x}\text{In}_x$ ($x = 0, 3, 6$ and 9 at. %) thin films. The intercepts of the straight lines with the photon energy axis give the values of the optical band gap, E_g .

In the low-absorption region ($\alpha \leq 10^4 \text{ cm}^{-1}$), the absorption coefficient α shows an exponential dependence on photon energy, $h\nu$, and obeys the Urbach relation [39]

$$\ln(\alpha) = \ln(\alpha_0) + \left(\frac{h\nu}{E_e}\right), \quad (10)$$

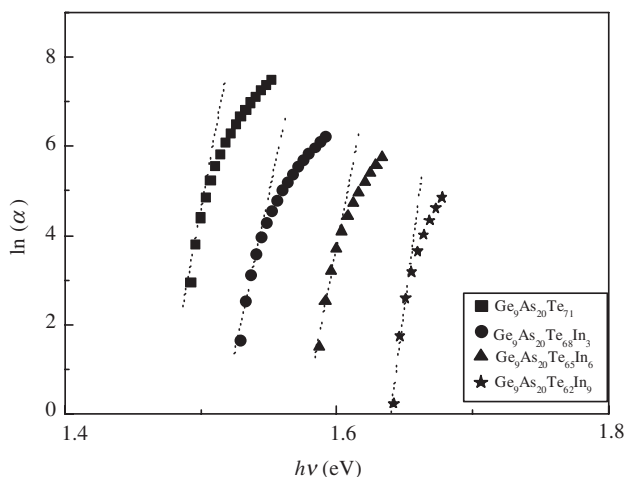


Figure 8. Dependence of $\ln(\alpha)$ on photon energy ($h\nu$) for the different composition of amorphous $\text{Ge}_9\text{As}_{20}\text{Te}_{71-x}\text{In}_x$ ($x=0, 3, 6$ and 9 at. %) films, from which the band tail energy, E_e , is estimated (Urbach's extrapolation).

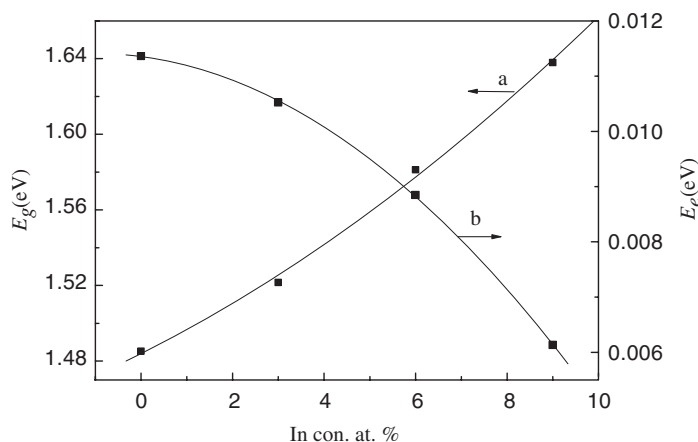


Figure 9. Optical band gap, E_g , and width of localized states, E_e , as a function of In content for different compositions of $\text{Ge}_9\text{As}_{20}\text{Te}_{71-x}\text{In}_x$ ($x=0, 3, 6$ and 9 at. %) films.

where α_0 is a constant and E_e is the Urbach energy (the width of the conduction or valence band tail of localized states, whichever is the larger). Figure 8 represents the plots of $\ln(\alpha)$ vs. $h\nu$ for the $\text{Ge}_9\text{As}_{20}\text{Te}_{71-x}\text{In}_x$ ($x=0, 3, 6$ and 9 at. %) thin films.

The deduced values of both of the optical band gap and the Urbach's energy as a function of In content are shown in Figure 9. From this figure one can note that, as the In content increases the E_g values increase while E_e values decrease. This increase in E_g values of amorphous films can be explained by a decreased tailing of the band, E_e into the gap [37,40].

The results obtained on the addition of In at the expense of Te atoms can be discussed in terms of the bonding character in the nearest-neighbor region [41],

which determines the electronic properties of semiconducting materials. A relevant parameter characterizing this is the average coordination number, N_r , which in our samples is defined by [42]

$$N_r = 4X_{\text{Ge}} + 3X_{\text{As}} + 2X_{\text{Te}} + 3X_{\text{In}}, \quad (11)$$

where X is the mole fraction of each element. Determination of N_r allows an estimation of the number of constraints, N_s . This parameter is closely related to the glass transition temperature and its related properties. We consider the constraint-counting argument originally proposed by Phillips for amorphous covalent materials [43]. Taking the short-range structure into account, Phillips has asserted that $N_s = N_d$, i.e. the number of topological constraints, N_s , evaluated for an atom is equal to the number of the flexibility, namely the spatial dimension, $N_d = 3$. For a material having the coordination number N_r , $N_s(N_r)$ can be expressed as a sum of radial, N^{α} , and angular, N^{β} , valence-force constraints [43–47]:

$$N_s = \frac{N_r}{2} + (2N_r - 3). \quad (12)$$

The calculated values of N_r , N_s , N^{α} and N^{β} for the $\text{Ge}_9\text{As}_{20}\text{Te}_{71-x}\text{In}_x$ ($x = 0, 3, 6$ and 9 at. %) films are listed in Table 3, using the values of N_r for Ge, As, Te and In [19,20] given in Table 1. It can be seen that all the parameters increase with increasing In content.

According to Pauling [48], the heat of atomization, $H_s(\text{AB})$, at standard temperature and pressure of a binary semiconductor formed from atoms A and B, is the sum of the heat of formation ΔH and the average of the temperatures of atomization, H_s^{A} and H_s^{B} , which corresponds to the average non-polar bond energy of the two atoms:

$$H_s(\text{AB}) = \Delta H + \frac{1}{2}(H_s^{\text{A}} + H_s^{\text{B}}). \quad (13)$$

The first term in Equation (13) is proportional to the square of the difference between the electronegativities, χ_{A} and χ_{B} , of the two atoms

$$\Delta H \propto (\chi_{\text{A}} - \chi_{\text{B}})^2. \quad (14)$$

This idea was extended to quaternary semiconductor compounds by Sadagopan and Gotos [30]. In most cases, the heat of formation of chalcogenide glasses is unknown. In the few materials for which it is known, its value does not exceed 10% of the heat of atomization and therefore can be neglected [49,50]. Hence, $H_s(\text{AB})$ is given quite well by

$$H_s(\text{AB}) = \frac{1}{2}(H_s^{\text{A}} + H_s^{\text{B}}). \quad (15)$$

The obtained results of the average heat of atomization for the present films are listed in Table 3, using the values of H_s for As, Se, Sb and Te given in Table 1.

The bond energies $D(AB)$ for heteronuclear bonds have been calculated using the empirical relation,

$$D(AB) = [D(AA)D(BB)]^{1/2} + 30(\chi_A - \chi_B)^2, \quad (16)$$

proposed by Pauling [51], where $D(AA)$ and $D(BB)$ are the energies of the homonuclear bonds (in units of kcal mol⁻¹) [29,31] and χ_A and χ_B are the electronegativity values for the involved atoms [29,32]. In the present compositions, the Ge–Te, As–Te and In–Te bonds will be the most favorable bonds to saturate all available valences of Te. After all these bonds are formed, there is still an unsatisfied Te valence, which must be resolved by the formation of Te–Te bonds, the proportion of which decreases with increase of the In content. As was explained, the glass transition behavior of amorphous systems can be expressed in terms of their cohesive energy (CE), which reflects the average bond strength, and at the same time allows the formation of bonds between like atoms, if there is an excess of a certain type of atom, until all available valences for the atoms are saturated. Based on the chemical-bond approach, the bond energies are assumed to be additive. Thus, the cohesive energies were estimated by summing the bond energies over all the bonds expected in the material.

The calculated values of the cohesive energies for all compositions are presented in Table 2. These results indicate that the cohesive energies of these glasses increase with increasing In content. It should be mentioned that the chemical-bond approach neglects dangling bonds and other valence defects as a first approximation. Also neglected are van der Waals interactions, which can provide a means for further stabilization via the formation of much weaker links than regular covalent bonds. It is suggested that the increase of E_g with increasing In content (Figure 9a) is most probably due to a reduction in the average stabilization energy. Concerning the values of the band tail width, E_e , it is seen that an increase of In content (i.e. an increase in CE) leads to a decrease in E_e (see Figure 9b). The increase of CE implies a higher bonding strength, i.e. a high E_g , and this means lower-energy defect bonds, which reduce the band tail width (see Figure 9).

The effect of In content on the optical gap E_g for Ge₉As₂₀Te_{71-x}In_x thin films is shown in Figure 9a (solid lines), from which one can observe that E_g increases with the In content. This variation can be described by an empirical formula as follows

$$E_g = 1.484 + 0.0122x - 0.00057x^2. \quad (17)$$

Also, the decrease in E_e with increasing In content can be described by the empirical relation (Figure 9b, solid line)

$$E_e = 0.0114 + 0.00012x - 0.000052x^2, \quad (18)$$

where x is the In content (at. %). The observed increase in E_g of amorphous films can be explained by a decreased degree of tailing of the bands into the gap [40,37]. From Figure 9 it can be seen that the values of E_e decrease as the In content increases. The Tauc model [52] based on electronic transitions between localized states in the band edge tails may well be valid for such systems.

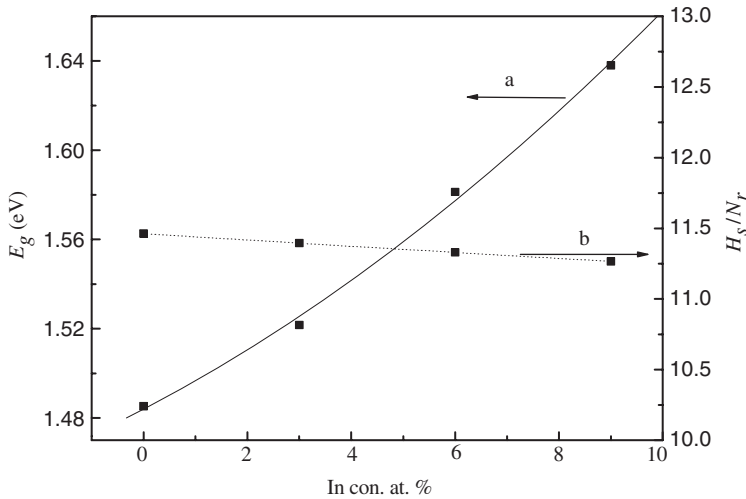


Figure 10. Optical band gap, E_g , and the parameter H_s/N_r as a function of In content for different compositions of $\text{Ge}_9\text{As}_{20}\text{Te}_{71-x}\text{In}_x$ ($x=0, 3, 6$ and 9 at. %) films.

Hurst and Davis [53] explained results of this type by suggesting that when the bond energies in the alloy are not very different, the increase in disorder associated with deviation from stoichiometry will tend to push the mobility edges further into the bands, thereby decreasing E_g . Furthermore, comparing E_g with H_s given in Table 3, we find that both E_g and H_s increase with increasing In content in our $\text{Ge}_9\text{As}_{20}\text{Te}_{71-x}\text{In}_x$ system. But according to Kastner [54,55], E_g for over constrained materials with higher connectivity, $4 \geq N_r \geq 3$, depends more strongly on H_s than for glasses with lower connectivity, $3 \geq N_r \geq 2$. This result suggests that the parameter H_s/N_r has a small effect on E_g , as confirmed in our study (see Figure 10).

5. Conclusions

An analysis proposed by Ruiz-Perez et al. [27], based on the use of the maxima and minima of interference fringes in reflectivity spectra, has been successfully applied to derive the real and imaginary parts of the complex index of refraction, the film thickness and the thickness variation of $\text{Ge}_9\text{As}_{20}\text{Te}_{71-x}\text{In}_x$ films. The wavelength dependence of the optical absorption in the films follows the Tauc's rule for the allowed non-direct transitions; with increasing In content the refractive index decreases while the optical band gap increases. The relationship between E_g and the chemical composition has been discussed in terms of chemical bonds, the cohesive energy, the average heat of atomization and the average coordination number. The dispersion of the refractive index has been discussed in terms of the single-oscillator Wemple–DiDomenico model. It was found that, the oscillator energy E_o is an average energy gap and, to a good approximation, scales with the optical band gap E_g , $E_o \approx 2E_g$. It is observed that the E_o values increase, whereas the refractive index $n(0)$ and the dispersion energy E_d decrease with increasing In content.

Acknowledgements

The author would like to thank Al-Azhar University for financial support. Also the author would like to thank Dr. A. Dahshan, Faculty of Science, Suez Canal University, Port Said, Egypt, for his help and advice throughout this work.

References

- [1] A.R. Hilton, D.J. Hayes and M.D. Rechin, *J. Non-Cryst. Solid.* 7 (1975) p.319.
- [2] J.A. Savage, *J. Non-Cryst. Solid.* 47 (1982) p.101.
- [3] A.B. Seddon, *J. Non-Cryst. Solid.* 44 (1995) p.184.
- [4] S.M. El-Sayed and G.A.M. Amin, *Vacuum* 62 (2001) p.353.
- [5] J. Rowlands and S. Kasap, *Phys. Today* 24 (1997) p.50.
- [6] A. Ganjoo, H. Jain, C. Yu, R. Song, J.V. Ryan, J. Irudayaraj, Y.J. Ding and C.G. Pantano, *J. Non-Cryst. Solid.* 352 (2006) p.584.
- [7] S.R. Ovshinsky, *Phys. Rev. Lett.* 21 (1968) p.1450.
- [8] C.B. Thomas, A.F. Frelt and J. Bonell, *Phil. Mag.* 26 (1972) p.617.
- [9] N. Lasocka and H. Matyja, *J. Non-Cryst. Solid.* 14 (1972) p.41.
- [10] A. Elshafie, B.A. Mansour and A. Abdel-All, *J. Phys. Chem. Solid.* 60 (1999) p.483.
- [11] A. Abdel-All, A. Elshafie and M.M. Elhawary, *Vacuum* 59 (2000) p.845.
- [12] P.E. Lippens, J.C. Jumas, J. Olivier-Fourcade, L. Aldon, A. Gheorghiu-de la Rocque and C. Sénémaud, *J. Phys. Chem. Solid.* 61 (2000) p.1761.
- [13] P.E. Lippens, J.C. Jumas, J. Olivier-Fourcade and L. Aldon, *J. Non-Cryst. Solid.* 271 (2000) p.119.
- [14] L. Aldon, P.E. Lippens, J.C. Jumas, J. Olivier Fourcade, H. Bemelmans and G. Langouche, *J. Non-Cryst. Solid.* 262 (2000) p.244.
- [15] J. Vázquez, C. Wagner, P. Villares and R. Jiménez-Garay, *Mater. Chem. Phys.* 58 (1999) p.187.
- [16] J.C. Manificier, J. Gasiot and J.P. Fillard, *J. Phys. E Sci. Instrum.* 9 (1976) p.1002.
- [17] R. Swanepoel, *J. Phys. E Sci. Instrum.* 16 (1983) p.1214.
- [18] R. Swanepoel, *J. Phys. E Sci. Instrum.* 17 (1984) p.896.
- [19] K.A. Aly, A. Dahshan and A.M. Abousehly, *Phil. Mag.* 88 (2008) p.47.
- [20] D.A. Minkov, *J. Phys. D Appl. Phys.* 22 (1989) p.1157.
- [21] J.M. González-Leal, E. Márquez, A.M. Bernal-Oliva and R. Jiménez-Garay, *Bol. Soc. Esp. Cerám. Vidrio* 36 (1997) p.282.
- [22] J.J. Ruiz-Pérez and E. Márquez, *Nuevos Métodos de Caracterización Óptica de Semiconductores Basados en Medidas Espectrópicas de Reflexión*, Ministerio de Defensa, Secretaria General Técnica, Madrid, 1997.
- [23] V.V. Filippov, *Optic Spectros.* 88 (2000) p.581.
- [24] J.J. Ruiz-Pérez, J.M. González-Leal, D.A. Minkov and E. Márquez, *J. Phys. D Appl. Phys.* 34 (2001) p.2489.
- [25] E. Márquez, J.M. González-Leal, R. Jiménez-Garay, S.R. Lukic and D.M. Petrovic, *J. Phys. D Appl. Phys.* 30 (1997) p.690.
- [26] E. Márquez, P. Nagels, J.M. González-Leal, A.M. Bernal-Oliva, E. Sleenckx and R. Callaerts, *Vacuum* 52 (1999) p.55.
- [27] J.J. Ruiz-Pérez, E. Márquez, D. Minkov, J. Reyes, J.B. Ramirez-Malo, P. Villares and R. Jiménez-Garay, *Phys. Scripta* 53 (1996) p.76.
- [28] L. Tichy and H. Ticha, *J. Non-Cryst. Solid.* 189 (1995) p.141.
- [29] S.S. Fouad, *Physica B* 270 (1999) p.360.
- [30] V. Sadagopan and H.C. Gotos, *Solid State Electron.* 8 (1965) p.529.

- [31] L. Tichy, A. Triska, H. Ticha, M. Frumar and J. Klikorka, *Solid State Comm.* 41 (1982) p.751.
- [32] J. Bicerano and S.R. Ovshinsky, *J. Non-Cryst. Solid.* 74 (1985) p.75.
- [33] T.S. Moss, *Optical Properties of Semiconductors*, Butterworths, London, 1959.
- [34] S.H. Wemple and M. DiDomenico, *Phys. Rev. B* 3 (1971) p.1338.
- [35] K. Tanaka, *Thin Solid Films* 66 (1980) p.271.
- [36] G. Kumar, J. Thomas, N. George, B. Kumar, P. Shnan, V. Npoori, C. Vallabhan and N. Unni Krishnan, *Phys. Chem. Glasses* 41 (2001) p.89.
- [37] E.A. Davis and N.F. Mott, *Phil. Mag.* 22 (1970) p.903.
- [38] H. Fritzsche, *Phil. Mag. B* 68 (1993) p.561.
- [39] F. Urbach, *Phys. Rev.* 92 (1953) p.1324.
- [40] P. Nagel, L. Tichy and A. Triska, *J. Non-Cryst. Solid.* 59–60 (1983) p.1015.
- [41] A.F. Ioffe and A.R. Regel, *Prog. Semicond.* 4 (1960) p.239.
- [42] N. Yamaguchi, *Phil. Mag.* 51 (1985) p.651.
- [43] J.C. Phillips, *J. Non-Cryst. Solid.* 34 (1979) p.153.
- [44] G.H. Dähler, R. Dandoloﬀ and H. Bilz, *J. Non-Cryst. Solid.* 42 (1980) p.87.
- [45] M.K. Rabinal, K.S. Sangunni and E.S.R. Gopal, *J. Non-Cryst. Solid.* 188 (1995) p.98.
- [46] M.F. Thorpe, *J. Non-Cryst. Solid.* 57 (1983) p.355.
- [47] A.A. Othman, K.A. Aly and A.M. Abousehly, *Thin Solid Films* 515 (2007) p.3507.
- [48] L. Pauling, *J. Phys. Chem.* 58 (1954) p.662.
- [49] S.S. Fouad, *Vacuum* 52 (1999) p.505.
- [50] S.S. Fouad, A.H. Ammar and M. Abo-Ghazala, *Physica B* 229 (1997) p.249.
- [51] J. Pauling, *Nature of the Chemical Bond*, Cornell University Press, Ithaca, NY, 1960.
- [52] J. Tauc, in *The Optical Properties of Solids*, F. Abeles ed., North Holland, Amsterdam, 1970, p.227.
- [53] C. Hurst and E.A. Davis, in *Amorphous and Liquid Semiconductors*, J. Stuke and W. Brenig eds., Taylor and Francis, London, 1974, p.49.
- [54] M. Kastner, *Phys. Rev. Lett.* 28 (1972) p.355.
- [55] M. Kastner, *Phys. Rev. B* 7 (1973) p.5237.